ARTICLES

Journal of Semiconductors
(2019) 40, 072902
doi: 10.1088/1674-4926/40/7/072902

Stable single photon sources in the near C-band range above 400 K

Qiang Li[1, 2, #], Ji-Yang Zhou[1, 2, #], Zheng-Hao Liu[1, 2], Jin-Shi Xu[1, 2, †], Chuan-Feng Li[1, 2, †], and Guang-Can Guo[1, 2]

[1]CAS Key Laboratory of Quantum Information, University of Science and Technology of China, Hefei 230026, China

[2]CAS Center for Excellence in Quantum Information and Quantum Physics, University of Science and Technology of China, Hefei 230026, China

Abstract: The intrinsic characteristics of single photons became critical issues since the early development of quantum mechanics. Nowadays, acting as flying qubits, single photons are shown to play important roles in the quantum key distribution and quantum networks. Many different single photon sources (SPSs) have been developed. Point defects in silicon carbide (SiC) have been shown to be promising SPS candidates in the telecom range. In this work, we demonstrate a stable SPS in an epitaxial 3C-SiC with the wavelength in the near C-band range, which is very suitable for fiber communications. The observed SPSs show high single photon purity and stable fluorescence at even above 400 K. The lifetimes of the SPSs are found to be almost linearly decreased with the increase of temperature. Since the epitaxial 3C-SiC can be conveniently nanofabricated, these stable near C-band SPSs would find important applications in the integrated photonic devices.

Key words: single photon source; stable photoluminescence; silicon carbide; elevated temperature

Citation: Q Li, J Y Zhou, Z H Liu, J S Xu, C F Li, and G C Guo, Stable single photon sources in the near C-band range above 400 K[J]. *J. Semicond.*, 2019, 40(7), 072902. http://doi.org/10.1088/1674-4926/40/7/072902

1. Introduction

Single-photon sources (SPSs) are critical in quantum information science. They can be used for quantum key distribution (QKD) of secure communications, which are guaranteed by the no cloning theorem[1]. Compared with the QKD protocol using weak coherent pulses from attenuated lasers, the use of ideal single photons can lead to high data transfer rate and long secure distance[2]. On the other hand, indistinguishable single photons can be used for quantum simulation[3] and quantum computation[4]. Great interests have been attracted to the race of demonstrating quantum supremacy[5], in which Boson sampling provides an attractive candidate[6]. It requires a linear quantum network with SPSs and single-photon detection. An abundance of theoretical and experimental efforts have been done in this field[7]. Moreover, SPSs also play important roles in the investigation of fundamental quantum problems. The intrinsic correlations clearly emerges with the use of single photons, especially in the demonstration of quantum contextual correlations[8–10], which can exist in a single particle without the classical counterpart.

Many different kinds of SPSs have been investigated. Heralded single photons prepared from the spontaneous parametric down-conversion with lasers pumping a birefringent crystal are commonly used[11]. However, they are probabilistic, which are influenced by the vacuum and high-order terms. The other promising system is the quantum dots in pillar micro-cavities[12–14], which has shown high quality indistinguishability and has been used to demonstrate multiphoton boson sampling[15, 16]. These quantum dot systems usually require cryogenic temperatures, which makes greater overheads in the practical applications. Point defects in semiconductor material are also considered as SPSs, including diamond[17], zinc oxide (ZnO)[18] and silicon carbide (SiC)[19]. They are stable solid-state SPSs and can work at room temperature. Moreover, they can be conveniently integrated into nanophotonic devices.

Defects in SiC as single photon emitters are of particular interests. SiC is an important and widely-used material in advanced high power and high temperature electronics. Many different polytypes exist in SiC with the most commonly used polytypes being 3C, 4H and 6H, which are of broad optical transparency. Different kinds of point defects in SiC are characterized as SPSs, including Si vacancies (V_{Si})[20–24], divacancies ($V_{Si}V_C$)[25–27] and carbon antisite-vacancy pair ($C_{Si}V_C$)[28, 29]. Recently, telecom range SPSs are also reported in SiC[30]. However, for the practical use, the SPSs with the wavelength in the C-band range would cause the lowest loss in optical fibers and would be critical for QKD distribution and the connection between remote quantum computation nodes with fibers. Moreover, the practical application of SPSs is likely to work at elevated temperatures. The investigation of robust C-band range SPSs is therefore of practical importance.

In this work, we demonstrate SPSs in a high-purity layer of epitaxial 3C-SiC (100) on a silicon substrate. The emission center wavelength around 1400 nm locates in the near C-band range, which is characterized by a set of long pass filters. The optical properties of these SPSs are demonstrated, which are shown to be of high qualities. We then increase the environmental temperature of the SPSs and find that they are stable even above 400 K. The lifetime of the SPSs are found to almost linearly decrease with the increase of temperature. Our work provides high-temperature stable SPSs, which can be further used for practical quantum information processing.

2. Experimental setup

In our experiment, we use a 3C-SiC membrane with thick-

These authors contribute equally to this work.
Correspondence to: J S Xu, jsxu@ustc.edu.cn; C F Li, cfli@ustc.edu.cn
Received 30 APRIL 2019; Revised 26 MAY 2019.
©2019 Chinese Institute of Electronics

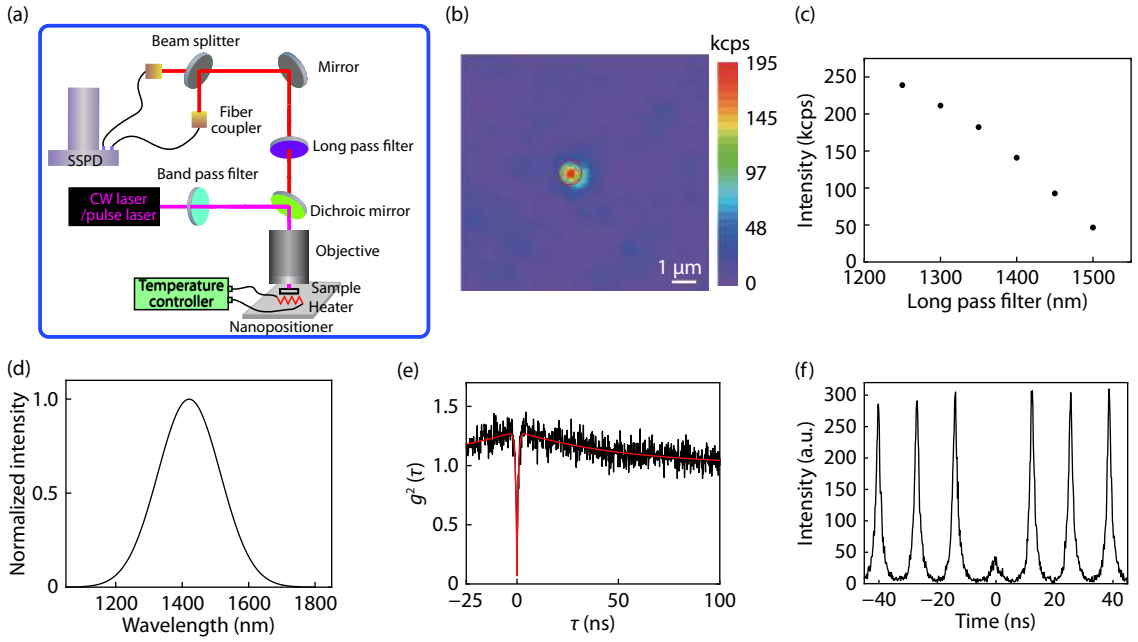

Fig. 1. (Color online) The experimental setup and the scanning image of the single photon emitter. (a) The experimental setup. The pump laser is focused by an objective to excite the sample mounted on a three-dimension nanopositioner stage. The temperature of the sample is controlled by a heater which is connected to a temperature controller. The emitted photons are filtered and then separated by a beam splitter, which are collected by fiber couplers and detected by superconducting single photon detectors (SSPD). (b) A $10 \times 10 \mu m^2$ confocal scan image on the surface of the sample under 0.5 mW laser excitation. A representative single photon emitter is denoted by the red circle. The scale bar is 1 μm. (c) The photon counts with the use of different long pass filters. (d) The reconstructed spectrum with the assumption of Gaussian distribution. (e) The second-order autocorrelation function of the corresponding SPS measured by the CW laser excitation. The black line is the corrected experimental result and the red line is the theoretical fitting using Eq. (1) with $g^2(0) = 0.06 \pm 0.03$. (f) The second-order autocorrelation function of the corresponding SPS under 50 μW pulsed laser excitation with a 76 MHz repetition rate.

ness of 4.1 μm epitaxial grown on a silicon substrate, which is purchased from NOVASIC Savoie Technolac. The 3C-SiC layers are grown in a chemical vapor deposition (CVD) system. The as received samples are immediately used in our sequential measurements after some cleaning processes without any implantation and annealing process. Fig. 1(a) shows our experimental setup. To locate the single point defect in the epitaxial 3C-SiC, we construct a home-built confocal microscopy. The pump laser is first filtered by a band pass filter. According to the purpose of the study, either a continuous wave (CW) laser with the center wavelength of 1064 nm or a pulse wave laser with the center wavelength at 1064 nm and a repetition rate of 76 MHz is used. After reflected by a dichroic mirror, the pump laser is focused by an oil objective (NA = 1.35) to excite the sample, which is mounted on a three-dimension nanopositioner stage. For the high temperature experiment, we use an objective with NA = 0.65 and the sample is mounted on a heater which is controlled by a temperature controller. The emitted fluorescence is filtered by a long pass filter. The photons are split by a beam splitter into two paths and collected by fiber couplers, which are then directed to superconducting single photon detectors (SSPD). The detected signals are sent to a time correlated single photon module (no shown in Fig. 1). By changing the time delay (τ) between these two paths, we can check the single-photon property of the fluorescence through the Hanbury-Brown and Twiss (HBT) interferometer and obtain the corresponding second-order photon correlation function $g^2(\tau)$.

3. Results and discussion

Fig. 1(b) shows a typical 10×10 μm^2 scanning image with the confocal microscopy system under 0.5 mW CW pumping. There is a bright emitter in the image, which is denoted by a red circle. To check the center wavelength of the fluorescence, we use a tomographic method to reconstruct the spectrum. Fig. 1(c) shows the corresponding intensities measured with the use of different long pass filters. Assuming the Gaussian distribution, the spectrum is reconstructed and shown in Fig. 1(d). The center wavelength of the fluorescence is deduced to be 1420 nm with a full width at half maximum (FWHM) of about 220 nm. The wavelength is closed to the C-band communication wavelength and would reduce the fiber loss. The fluorescence is then sent to the HBT interferometry. By changing the relative delay time τ, we obtain the second-order time correlation function $g^2(\tau)$. In order to reduce the influence of background signal and noise, we correct the raw $g^2_{\rm raw}(\tau)$ using the function of $g^2(\tau) = \left[g^2_{\rm raw}(\tau) - \left(1-\alpha^2\right)\right]/\alpha^2$, where $a = s/(s + b)$ with s being the signal counts and b being the background counts[22, 27, 30]. The corresponding $g^2(\tau)$ can then be fitted by the equation

$$g^2(\tau) = 1 - (1+\varepsilon)\mathrm{e}^{-\frac{|\tau|}{\gamma_1}} + a\mathrm{e}^{-\frac{|\tau|}{\gamma_2}}, \quad (1)$$

where ε, γ_1 and γ_2 are laser power-dependent parameters. $g^2(\tau)$ under the CW pumping is shown in Fig. 1(e) with the dip fitting to be 0.06 ± 0.03, which shows the high quality of the room temperature SPS. We further investigate the $g^2(\tau)$ under

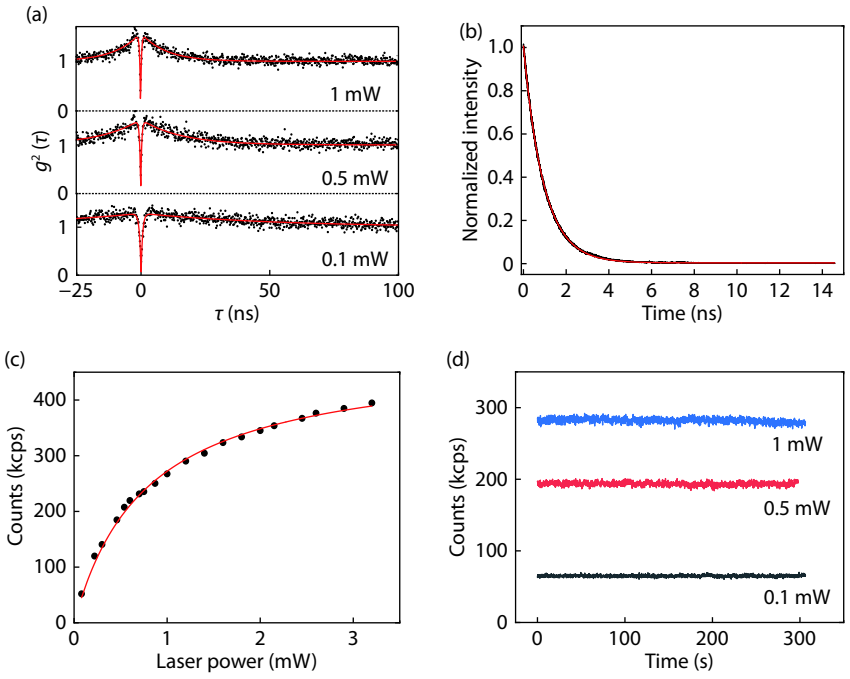

Fig. 2. (Color online) Optical properties of the SPS at room temperature. (a) The second-order correlation function $g^2(\tau)$ at different pump powers. (b) The life-time measurement. The black line is the experimental result and the red line is the single-exponential fitting. (c) The saturation behavior. Black dots are the experimental results and the red line is the theoretical fitting. (d) The stability of the counting rates at different pump power. The sampling time is 0.1 s. No photon bleaching or photon blinking is observed.

the excitation of a pulse laser with 76 MHz repetition rate, which is shown in Fig. 1(f). The value of the dip at the zero delay time is well below 0.5 with the value of $g^2(0) = 0.229 \pm 0.004$, which further confirms the high quality of the room temperature SPS.

We then investigate the optical properties of this SPS. A set of power-dependent $g^2(\tau)$ functions are measured. The representative experimental results with 0.1, 0.5 and 1 mW pumping are shown in Fig. 2(a). The red solid lines are the fittings using Eq. (1). The obvious photon-bunching effect in the second-order time correlation function with high power pumping implies the existence of a metastable state. Therefore, a three-level system model can be used to describe the observed single photon emitter[28–31]. We further investigate the life-time of the SPS using the pulse laser which is separated into two parts. One of them is used as a trigger and the other is used to excite the SPS. The detected normalized intensity $I(t)$ (black line) is shown in Fig. 2(b) with the red line showing the single-exponential fitting $I(t)\exp(-t/\tau)$. The life time is then deduced to be 0.942 ± 0.001 ns. By increasing the power of the pump laser, the counting rate increases accordingly. Fig. 2(c) shows the counting rates as a function of the pump power. Black dots are experimental results and the red line is the fitting using the power dependence model $I(P) = I_s/(1 + P_0/P)$. The maximal emission counts (I_s) is deduced to be 484 kcps at the saturation power of about 0.78 mW. Stable SPSs are important in practical applications. We then test the stability of the SPS under different pump powers. The experimental results are shown in Fig. 2(d). The sampling time is 0.1 s. No photon bleaching or photon blinking is observed at the excitation power of 0.1, 0.5 and 1 mW, in which the counting rates remain almost the same in 5 min.

We further investigate the temperature influences. In this case, the objective is changed to the one with NA = 0.65. A typical 20×20 μm^2 scan image is shown in Fig. 3(a) with the single photon emitter denoted by the red circle. The emitted photons are detected with different long pass filters. The corresponding photon counts are shown in Fig. 3(b). The spectrum is then deduced to be at a central wavelength of 1385 nm with a FWHM of 155 nm. The sample is heated by a heater, in which the temperature is controlled by a temperature controller. The counting rates are stable and keep almost the same when the temperature increases above 400 K. Several typical experimental results are shown in Fig. 3(c). The sampling time is set to be 0.1 s. We do not find any photon bleaching and photon blinking. The $g^2(\tau)$ at the corresponding temperature are further measured. Three representative results are shown in Fig. 3(d). The values of $g_2(0)$ fitting from the data of 296, 346 and 406 K are 0.06 ± 0.04, 0.06 ± 0.05 and 0.20 ± 0.03, respectively. All the dips are well lower than 0.5, which confirm the single photon emission. The stability of the SPSs even at high temperature would found important practical applications.

As shown in Fig. 3(d), The width of $g^2(\tau)$ becomes smaller when the temperature increases. It implies the decrease of the corresponding lifetime. This observation is further confirmed by the detailed results of the dependence of the lifetime on temperature, which is shown in Fig. 4(a). The lifetime at room temperature is measured to be about 3.35 ns and the lifetime is reduced to be about 1.31 ns at 403 K. A representative lifetime measurement is shown in Fig. 4(b). This property is different from that observed in the two-dimensional hBN[32], in which the lifetimes of defect single photon emitters were found to remain the same when the temperature increases. Further investigations are needed to completely understand this phenomenon.

4. Conclusion

In conclusion, we have demonstrated SPSs in near C-band wavelengths in a high-purity epitaxial 3C-SiC layer grown on a

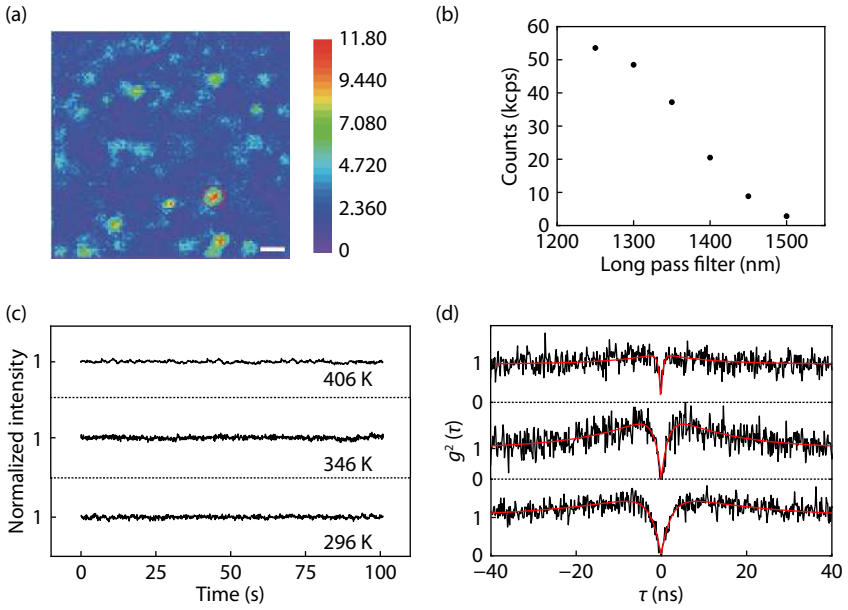

Fig. 3. (Color online) The optical properties at elevated temperatures. (a) A 20 × 20 μm^2 confocal scan image on the surface of the sample under 0.5 mW laser excitation with an objective NA = 0.65. A representative single photon emitter is denoted by the red circle. (b) The photon counts with the use of different long pass filters. (c) The stability of the counting rates at different temperature. The sampling time is 0.1 s. No photon bleaching or photon blinking is observed at even 406 K. (d) The corresponding $g^2(\tau)$ at the corresponding temperature.

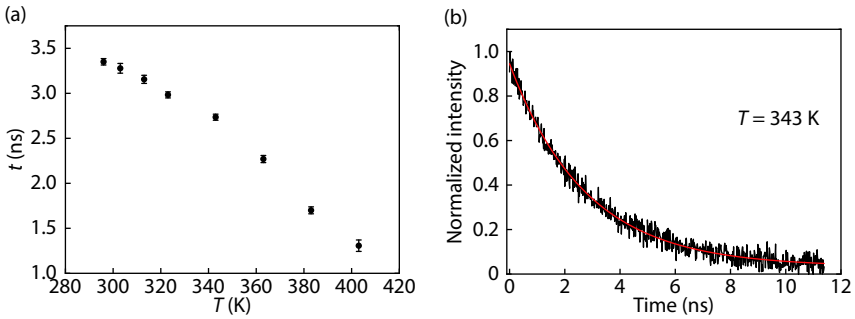

Fig. 4. (Color online) The dependence of lifetime on temperature. (a) The lifetime of the single photon emitter as a function of temperature. With the increase of the temperature, the lifetime almost linearly decreases. (b) The representative lifetime measurements at temperature 343 K.

Si substrate. The wavelength matches the requirement of optical fiber transmission and would found important applications in future QKD and remote quantum network. The SPSs are shown to be stable from room temperature to above 400 K, which are suitable for practical applications with elevated temperature. However, this type of the single photon source described in the paper is different from the previously discovered intrinsic defects in 3C-SiC[26, 33], and the origin is still unknown. Further researches and confirmations for the origin of the SPSs are proposed to be of great importance for controllably preparing the SPSs and improving the qualities of them. Moreover, the lifetime of SPSs is found to almost linearly decrease with the increase of the surrounding temperature, which can be used for full-optical temperature sensing. Further investigations are needed to completely understand this phenomenon. By using a vacuum chamber[32], the properties of SPSs can be investigated at higher temperatures. Moreover, the epitaxial 3C-SiC is suitable for nanophotonic fabrications. Different kinds of photonic structures, such as photonic crystals[34, 35] and bullseye gratings[36–38] can be conveniently fabricated, which can be further used to increase the brightness of the SPSs. Recently, the electrically driven visible SPSs have been found in SiC[39, 40], which greatly enhances the feasibility to integrate SPSs into complex architectures. Further investigations on electrically driven C-band SPSs in thin 3C-SiC membranes are of particular importance, which would find practical applications in quantum information processing.

Acknowledgment

This work was supported by the National Key Research and Development Program of China (Grant No. 2016YFA0302700), the National Natural Science Foundation of China (Grants No. 61725504, 61327901, 61490711, 11821404 and 11774335), the Key Research Program of Frontier Sciences, Chinese Academy of Sciences (CAS) (Grant No. QYZDY-SSW-SLH003), Anhui Initiative in Quantum Information Technologies (AHY060300 and AHY020100), the Fundamental Research Funds for the Central Universities (Grant Nos.

WK2030380017 and WK2470000026). This work was partially carried out at the USTC Center for Micro and Nanoscale Research and Fabrication.

References

[1] Wootters W K, Zurek W H. A single quantum cannot be cloned. Nature, 1982, 299(5886), 802

[2] Scarani V, Bechmann-Pasquinucci H, Cerf N J, et al. The security of practical quantum key distribution. Rev Mod Phys, 2009, 81(3), 1301

[3] Aspuru-Guzik A, Waither P. Photonic quantum simulators. Nat Phys, 2012, 8(4), 285

[4] Kok P, Munro W J, Nemoto K, et al. Linear optical quantum computing with photonic qubits. Rev Mod Phys, 2007, 79(1), 135

[5] Preskill J. Quantum computing and the entanglement frontier. arXiv: 1203.5813v3, 2012

[6] Aaronson S, Arkhipov A. The computational complexity of linear optics. Proceedings of the ACM Symposium on Theory of Computing, ACM, New York, 2011, 333

[7] Lund A P, Bremner M J, Ralph T C. Quantum sampling problems, Boson sampling and quantum supremacy. npj Quantum Inform, 2017, 3, 15

[8] Lapkiewicz R, Li P, Schaeff C, et al. Experimetnal non-classicality of an indivisible quantum system. Nature, 2011, 474(7352), 490

[9] Xiao Y, Xu Z P, Li Q, et al. Experimental observation of quantum state-independent contextuality under no-signaling conditions. Opt Express, 2018, 26(1), 32

[10] Xiao Y, Xu Z P, Li Q, et al. Experimental test of quantum correlations from platonic graphs. Optica, 2018, 5(6), 718

[11] Kwiat P G, Mattle K, Weinfurter H, et al. New high-intensity source of polarization- entangled photon pairs. Phys Rev Lett, 1995, 75(24), 4337

[12] Gazzano O, Michaelis de Vasconecellos S, Arnold C, et al. Bright solid-state sources of indistinguishable single photons. Nat Commun, 2013, 4, 1425

[13] He Y M, He Y, Wei Y J, et al. On-demand semiconductor single-photon source with near-unity indistinguishability. Nat Nanotechnol, 2013, 8(3), 213

[14] Santori C, Fattal D, Vuckovic J, et al. Indistinguishable photons from a single-photon device. Nature, 2002, 419(6907), 594

[15] Wang H, He Y, Li Y H, et al. High-efficiency multiphoton boson sampling. Nat Photon, 2017, 11(6), 361

[16] Loredo J C, Broome M A, Hilaire P, et al. Boson sampling with single-photon fock states from a bright solid-state source. Phys Rev Lett, 2017, 118(13), 130503

[17] Jelezko F, Wrachtrup J. Single defect centres in diamond: A review. Phys Status Solidi A, 2006, 203(13), 3207

[18] Morfa A J, Gibson B C, Karg M, et al. Single-photon emission and quantum characterization of zinc oxide defects. Nano Lett, 2012, 12(2), 949

[19] Lohrmann A, Johnson B C, McCallum J C, et al. A review on single photon sources in silicon carbide. Rep Prog Phys, 2017, 80(3), 034502

[20] Wang J, Zhou Y, Zhang, X, et al. Efficient generation of an array of single silicon-vacancy defects in silicon carbide. Phys Rev Appl, 2017, 7(6), 064021

[21] Widmann M, Lee S Y, Rendler T, et al. Coherent control of single spins in silicon carbide at room temperature. Nat Mater, 2015, 14(2), 164

[22] Fuchs F, Stender B, Trupke M, et al. Engineering near-infrared single-photon emitters with optically active spins in ultrapure silicon carbide. Nat Commun, 2015, 6, 7578

[23] Lienhard B, Schröder T, Mouradian S, et al. Bright and photostable single-photon emitter in silicon carbide. Optica, 2016, 3(7), 768

[24] Radulaski M, Widmann M, Niethammer M, et al. Scalable quantum photonics with single color centers in silicon carbide. Nano Lett, 2017, 17(3), 1782

[25] Christle D J, Falk A L, Andrich P, et al. Isolated electron spins in silicon carbide with millisecond coherence times. Nat Mater, 2015, 14(2), 160

[26] Falk A L, Buckley B B, Calusine G, et al. Polytype control of spin qubits in silicon carbide. Nat Commun, 2013, 4, 1819

[27] Christle D J, Klimov P V, Charles F, et al. Isolated spin qubits in SiC with a high-fidelity infrared spin-to-photon interface. Phys Rev X, 2017, 7(2), 021046

[28] Castelletto S, Johnson B C, Zachreson C, et al. Room temperature quantum emission from cubic silicon carbide nanoparticles. ACS Nano, 2014, 8(8), 7938

[29] Castelletto S, Johnson B, Ivády V, et al. A silicon carbide room-temperature single-photon source. Nat Mater, 2014, 13(2), 151

[30] Wang J, Zhou Y, Wang Z, et al. Bright room temperature single photon source at telecom range in cubic silicon carbide. Nat Commun, 2018, 9, 4106

[31] Neu E, Steinmetz D, Riedrich-Möller J, et al. Single photon emission from silicon-vacancy colour centres in chemical vapour deposition nano-diamonds on iridium. New J Phys, 2011, 13, 025012

[32] Kianinia M, Regan B, Abdulkader S, et al. Robust solid-state quantum system operating at 800 K. ACS Photon, 2017, 4(4), 768

[33] Radulaski M, Babinec T M, Mueller K, et al. Visible photoluminescence from cubic (3C) silicon carbide microdisks coupled to high quality whispering gallery modes. ACS Photon, 2015, 2(1), 14

[34] Schell A W, Neumer T, Shi Q, et al. Laser-written parabolic microantennas for efficient photon collection. Appl Phys Lett, 2014, 105(23), 231117

[35] Wan N H, Shields B J, Kim D, et al. Efficient extraction of light from a nitrogen-vacancy center in a diamond parabolic reflector. Nano Lett, 2018, 18(5), 2787

[36] Choy J T, Bulu I, Hausmann B J, et al. Spontaneous emission and collection efficiency enhancement of single emitters in diamond via plasmonic cavities and gratings. Appl Phys Lett, 2013, 103(16), 161101

[37] Li L, Chen E H, Zheng J, et al. Efficient photon collection from a nitrogen vacancy center in a circular bullseye grating. Nano Lett, 2015, 15(3), 1493

[38] Livneh N, Harats M G, Yochelis S, et al. Efficient collection of light from colloidal quantum dots with a hybrid metal–dielectric nanoantenna. ACS Photon, 2015, 2(12), 1669

[39] Lohrmann A, Iwamoto N, Bodrog Z, et al. Single-photon emitting diode in silicon carbide. Nat Commun, 2015, 6, 7783

[40] Sato S, Honda T, Makino T, et al. Room temperature electrical control of single photon sources at 4H-SiC surface. ACS Photon, 2018, 5(8), 3159